Cooperative Motion Control Using Hybrid Acoustic-Optical Communication Networks ⋆

Rodrigo Rego * **Nguyen Hung** * **Antonio Pascoal** *

* *Laboratory of Robotics and Systems in Engineering and Science(LARSyS), ISR/IST, University of Lisbon, Lisbon, Portugal* {*rodrigorego, nguyen.hung, antonio*}*@tecnico.ulisboa.pt.*

Abstract: There is currently widespread interest in the development of groups of autonomous underwater vehicles for ocean exploration. This calls for the deployment of robots that can act in cooperation by exchanging data over communication networks. For this purpose, acoustic networks have been so far the choice par excellence. However, for operations involving vehicles operating at close range, there is currently a flurry of activity on the use of optical-based communication systems, capable of higher transmission rates. As a result, the goal of this work is to make optical communications viable and to use both communication technologies during underwater cooperative missions. Motivated by this goal, the first part of this work is dedicated to design a coordination controller with an event-based communication strategy for the coordination of the vehicles over the acoustic network. The second part of this work proposes an algorithm to make optical communications viable, which ultimately boils down to achieving optical beam alignment between a pair of cooperative agents. The proposed algorithm is illustrated by simulation results that show optical beam alignment being reached for a pair of vehicles in a cooperative formation.

Keywords: Motion Control, Cooperative Path Following, Autonomous Underwater Vehicles, Acoustic, Optical Communication, Event-Triggered Communications

1. INTRODUCTION

Acoustic systems are the pervasive solution to underwater communications, but their price is quite high and transmissions rates low. For this reason, there is currently considerable interest in the possible use of optical modems, as affordable units with the capability to transmit data at higher rates Gois et al. [2016]. Optical communication systems have, however, narrow directivity patterns, posing a challenge to achieve optical beam alignment while steering the vehicles.

As a result, the emphasis of this work lies in the development of algorithms for cooperative maneuvers, using data exchanged among the vehicles, by resorting to acoustic modems, when the vehicles are distant from each other and to broadcast their coordination states, and optical modems, when the vehicles operate at close range. In the latter case, the optical modems can also serve the dual purpose of transferring large volumes of data from one vehicle to another.

1.1 Topic Overview

Cooperative motion control of multiple autonomous marine vehicles (AMVs) has been receiving widespread interest over the last decade. This is motivated by the need to resort to the utilization of groups of AMVs for scientific activities and commercial applications where the use of a single vehicle may prove inefficient or lack robustness. An example of these types of scenarios arises in the scope of the WiMUST project where a group of cooperative AMVs is controlled to maneuver along a desired geometrical formation, to perform geotechnical acoustic surveys at sea Simetti et al. [2021]. Another example can be found in Abreu et al. [2015] where a set of heterogeneous AMVs acts in a cooperative manner for data acquisition and habitat mapping in complex underwater 3D environments such as canyons and rugged cliff areas.

To achieve cooperation among the vehicles, communication plays a vital role. In underwater environments, acoustic sound is the mainstream communication technology because it can operate at long ranges (up to thousands of meters), while other technologies such as radio frequency (RF) or optical are often limited to tenths of meters Gois et al. [2016]. However, acoustic signals are severely distorted by extensive multipath and broadband Doppler, on top of having a long propagation delay and low bandwidth. Recent work in optical communications (see in Gois et al. [2016]) shows that the latter can be a potential complementing solution to acoustic communications in applications where the vehicles operate at short range and require high data rate transmission. The main challenge with optical communications is that optical links are directive and require strategies for keeping correct alignment at the channel endpoints.

Motivated by the above considerations, this paper proposes a simple cooperative control architecture for multiple AMVs that uses a hybrid acoustic-optical communications network. The main objective is to exploit advantages of both communication technologies. That is, acoustic

⋆ This research was partially supported by the H2020 EU Marine Robotics Research Infrastructure Network (Project ID 731103), the H2020-EU.1.2.2 - FET Proactive RAMONES project (Grant agreement ID: 101017808), and the LARSYS - UIDP/500009/2020, with funding from Fundação para a Ciência e Tecnologia (FCT). The second author benefited from a PhD scholarship provided by IST.

modems are used when the vehicles are distant from each other and to always broadcast the vehicles' states, while optimal modems are used for communications among the vehicles at short range. Since acoustic communications are expensive and have low bandwidth, we apply an event-triggered communication (ETC) method, developed in Hung et al. [2019], to reduce the communications frequency. We also propose a simple "sweeping technique" to make the optical beams align so as to make the optical modems receive maximal signal power.

2. OVERVIEW OF THE COOPERATIVE CONTROL SYSTEM PROPOSED

The cooperative motion control scenario adopted in the present paper follows the concept of cooperative path following (CPF) presented in Ghabcheloo et al. [2009], Rego et al. [2019], Hung et al. [2020]. In the context of CPF, each vehicle is assigned with a spatial path to follow meanwhile it also coordinates with its neighboring vehicles over a (acoustic) communication network so as to position itself relative to its neighbors in a desired geometrical formation. Fig. 1 illustrates, at the abstract level, the overall control system implemented in each vehicle. Details of this control system are described next.

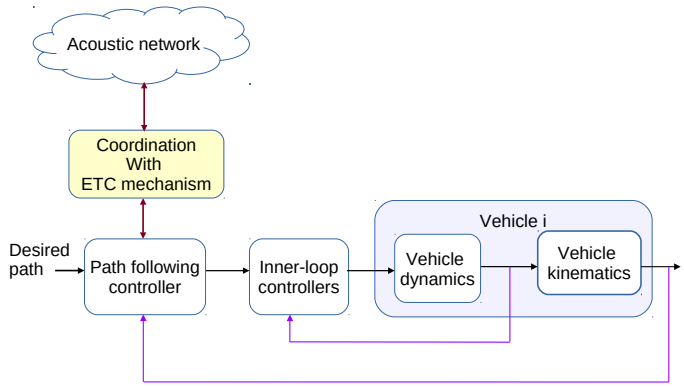

Fig. 1. Overall control system for each vehicle i.

2.1 Vehicle's model

In this work, we adopt the model of MEDUSA class underwater vehicle developed at IST. The vehicle's outlook is shown in Fig. 2 while its specification can be found in Abreu et al. [2016]. For simplicity of exposition we assume that the vehicle only maneuvers in the horizontal $x_I - y_I$ plane.

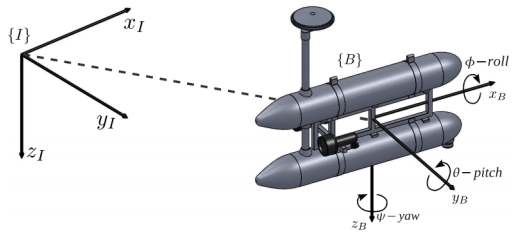

Fig. 2. MEDUSA class autonomous underwater vehicle (source: Ribeiro [2011])

In what follows, the inertial North-East (NE) frame is denoted by $\{I\} = \{x_I, y_I\}$, where the axis x_I points North, and the axis y_I points East. Let M be the center of mass of the vehicle and let the position of M in $\{I\}$ be denoted by $\boldsymbol{p} = [x, y]^{\mathrm{T}} \in \mathbb{R}^2$. Let also $\{B\} = \{x_B, y_B\}$ be a body-fixed frame whose origin is attached at M. In addition, denote by $\boldsymbol{v} = [u, v]^{\mathrm{T}} \in \mathbb{R}^2$ the vehicle's velocity vector expressed in $\{B\}$ where u, v are the surge and sway speeds, respectively. Furthermore, it is assumed that the vehicle's sway motion is too small so that it can be negligible, that is, making $v = 0$ (see Abreu et al. [2016]) and yielding the following simplified kinematic model

$$\begin{aligned} \dot{x} &= u\cos(\psi) \\ \dot{y} &= u\sin(\psi) \\ \dot{\psi} &= r, \end{aligned} \tag{1}$$

where ψ is the vehicle heading/yaw and r is its heading/yaw rate.

Regarding the vehicle dynamics model, we used the 3-DOF model described in Fossen [2011] where the model's parameters are specified in Rego [2021].

2.2 Inner-loop controllers

The inner-loop controllers are responsible for tracking references of the vehicle speed and heading rate generated by the path following controller. In our work, the speed controller is tracked by a proportional-integral (PI) controller while the heading rate controller is tracked by a linear-quadratic regulator (LQR) controller. The LQR is designed based on a model resulted from a linearization around the origin and considering a constant velocity of operation. Due to the space limitation, we refer to Rego [2021] for the process of design of the inner-loop controllers.

2.3 Path following controller

The path following controller follows the work in Lapierre et al. [2006] whose concept is illustrated in Fig. 3. Let $\{C\}$ be the path parameterized by its arc-length s, given by

$$\boldsymbol{p}_{\mathrm{d}}(s) = [x_{\mathrm{d}}(s), y_{\mathrm{d}}(s)] \in \mathbb{R}^2. \tag{2}$$

Let P be a generic point on the path whose coordinate is given by (2). In the path following method adopted, P plays the role of a *"reference point"* for the vehicle to track with respect to the path following objectives, defined as

(1) geometrical objective: make $\boldsymbol{p}(t) \to \boldsymbol{p}_{\mathrm{d}}(t)$ as $t \to \infty$,
(2) dynamics objective: $u(t) \to u_{\mathrm{d}}(t)$ as $t \to \infty$,

where u_{d} is the vehicle's desired speed profile. Let $\{T\}$ be a parallel-transport frame attached to P, making with x_I an angle θ_c and $[s_1, y_1]^T = R(\theta_c)(\boldsymbol{p} - \boldsymbol{p}_{\mathrm{d}})$ are the coordinates of M in $\{T\}$, where $R(\theta_c)$ is the rotation matrix from $\{I\}$ to $\{T\}$. Then, following the procedure in Lapierre et al. [2006] we obtain the path following error system, given by

$$\begin{cases} \dot{s}_1 = -\dot{s}\,(1 - c_c y_1) + u\cos(\theta) \\ \dot{y}_1 = -c_c \dot{s} s_1 + u\sin(\theta) \\ \dot{\theta} = r - c_c \dot{s} \end{cases} \tag{3}$$

where θ, defined as $\theta = \psi - \theta_c$, is the orientation error between the vehicle heading and the tangent of the path at P, which must be driven to zero as $t \to \infty$. Additionally, (s_1, y_1) must also be driven to zero as $t \to \infty$, making the vehicle approach the path. In order to meet these requirements, we adopt the control law, proposed in Lapierre et al. [2006], given by

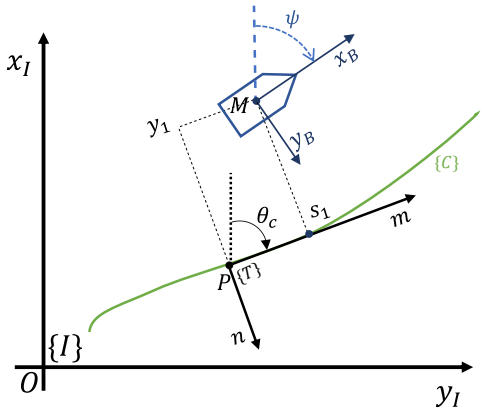

Fig. 3. Configuration for the L. Lapierre's guidance method.

$$\begin{aligned}\dot{s} &= u\cos\theta + k_1 s_1 \\ r &= \dot{\delta} + \gamma y_1 u \tfrac{\sin\theta - \sin\delta}{\theta - \delta} - k_2(\theta - \delta) + c_c \dot{s},\end{aligned} \tag{4}$$

where k_1, k_2, γ are positive gains. It is important to note that in order to fulfill the dynamics objective the vehicle's speed is assigned as the desired speed profile, that is,

$$u = u_{\mathrm{d}}. \tag{5}$$

It is proven in Lapierre et al. [2006] that these control laws yield global convergence of the vehicle's path to the desired path, thus achieving path following.
In next section, we describe the cooperative controller and event-triggered communication mechanism which are the main focus of the present paper.

3. MULTIPLE VEHICLE COORDINATION CONTROL

Coordination control between vehicles is to be achieved through the design of a coordination controller that drives a certain coordination error to zero. In the context of the present paper, the normalized arc-lengths of the paths, denoted by $\gamma^{[i]}$ are considered as the coordination states, given by

$$\gamma^{[i]} = s^{[i]}/L^{[i]}. \tag{6}$$

where $s^{[i]}, L^{[i]}$ correspond to the arc-length and total path length of path i, respectively. Given the path following control law in (4) it follows that

$$\dot{\gamma}^{[i]} = (u^{[i]}\cos\theta^{[i]} + k_1 s_1^{[i]})/L^{[i]}. \tag{7}$$

Suppose that for the time being the vehicles already stayed on their paths (i.e. $\theta^{[i]} = 0, s_1^{[i]} = 0, \forall i$), thus the above equation can be simplified as

$$\dot{\gamma}^{[i]} = u^{[i]}/L^{[i]}. \tag{8}$$

Let $\mathcal{N}^{[i]}$ be the set of neighbors of vehicle i where i can get information from. The coordination control problem is stated as follows.
Coordination Problem: *Consider a network of multiple vehicles where the dynamics of the coordination states are given by* (8)*. Derive a control law for* $u^{[i]}(\gamma^{[i]}, \gamma^{[j]}), j \in \mathcal{N}^{[i]}$ *such that* $\gamma^{[i]}(t) - \gamma^{[j]}(t) \to 0, \forall i, j$ *and* $\dot{\gamma}^{[i]}(t) \to u_L, \forall i$ *as* $t \to \infty$*, where* u_L *is the normalized desired speed of the formation.*
It was shown in Hung et al. [2019] and Hung et al. [2020] that if the graph induced by the vehicle network is undirected and connected then the coordination problem is solved with the control law given by

$$u^{[i]} = L^{[i]}(u_L + u_c^{[i]}), \tag{9}$$

where

$$u_c^{[i]} = -k_\xi \tanh\left(\sum_{j\in\mathcal{N}^{[i]}} \gamma^{[i]} - \gamma^{[j]}\right); i \in \mathcal{N} \tag{10}$$

and k_ξ is a positive constant. Above the hyperbolic tangent is used to bound $u_c^{[i]}$ in order to prevent the speed reference for the vehicle become negative.

3.1 Event-Triggered Communication Mechanism

In this section we describe an event-triggered communication (ETC) mechanism, in which the vehicles only need to exchange data with their neighbors when found necessary, in accordance with a properly defined criterion. The ETC mechanism follows the method proposed in Hung et al. [2020] and Hung et al. [2019] and is presented next.

In this mechanism, instead of using the true neighboring states, $\gamma^{[j]}; j \in \mathcal{N}^{[i]}$, the previously defined control law (10) uses their estimates – if any agent can produce good estimates of the neighboring states, then there is no need to communicate continuously. Letting $\hat{\gamma}^{[ij]}$ be an estimate of $\gamma^{[j]}$ computed by vehicle i (to be defined later) then in the context of ETC mechanism

$$u_c^{[i]} = -k_\xi \tanh\left(\sum_{j\in\mathcal{N}^{[i]}} \gamma^{[i]} - \hat{\gamma}^{[ij]}\right); i \in \mathcal{N}. \tag{11}$$

In order to compute $\gamma^{[ij]}$ vehicle i runs the estimator

$$\begin{aligned}\dot{\hat{\gamma}}^{[ij]}(t) &= u_L \\ \hat{\gamma}^{[ij]}\left(t_k^{[ij]}\right) &= \gamma^{[j]}\left(t_k^{[j]}\right),\end{aligned} \tag{12}$$

where for each generic i, $\left\{t_k^{[i]}\right\}; k \in \mathbb{N}$ is the sequence of time instants at which vehicle i sends its current value of $\gamma^{[i]}(t_k^{[i]})$ to its neighbors. In order to monitor how well the neighbors predict its coordination state, vehicle j also runs an estimator, given by

$$\begin{aligned}\dot{\hat{\gamma}}^{[j]}(t) &= u_L \\ \hat{\gamma}^{[j]}\left(t_k^{[j]}\right) &= \gamma^{[j]}\left(t_k^{[j]}\right).\end{aligned} \tag{13}$$

The second equation (13) implies that whenever vehicle j broadcasts $\gamma^{[j]}$ to its neighbors, the initial condition for $\hat{\gamma}^{[j]}$ will be reset.
Equations (12) and (13) imply that if without communication delays then $\hat{\gamma}^{[ij]}(t) = \hat{\gamma}^{[j]}(t)$ for all t, thus

$$e^{[ij]} := \hat{\gamma}^{[ij]} - \gamma^{[j]} = \hat{\gamma}^{[j]} - \gamma^{[j]} =: e^{[j]}$$

for all j. In other words, the vehicles know how well their neighbors predict their coordination states.

Having defined the new distributed control law, which considers the estimates of the states, the next step is to define the triggering function that dictates when the vehicles broadcast their coordination sates.

3.2 Time-Dependent Triggering Events

For a purely time-dependent triggering event, to ensure that the estimation error is bounded, vehicle i should transmit $\gamma^{[i]}$ whenever $e^{[i]}$ hits a designed threshold $\eta^{[i]}$ that is dependent on time, where recall that $e^{[i]}(t) = \hat{\gamma}^{[i]}(t) - \gamma^{[i]}(t)$ is the local estimation error of vehicle i itself. The triggering function for vehicle i is given by

$$h^{[i]}(t) = \left|e^{[i]}(t)\right| - \eta^{[i]}(t), \tag{14}$$

where $\eta^{[i]}(t)$ belongs to a class of non-negative functions $\mathcal{C}$ defined by $\mathcal{C} := \{f : R_{\geq 0} \to R_{\geq 0} \mid 0 \leq f(t) \leq c_u\}$ for all $i \in \mathcal{N}$. For example, $\eta^{[i]}(t) = c_1 + c_2 e^{-\alpha t}$ with a proper choice of c_1, c_2 and α is a typical function belonging to $\mathcal{C}$. With this definition, vehicle i will send its state to its neighbors whenever $h^{[i]}(t) \geq 0$.

3.3 State-Dependent Triggering Events

Regarding state-dependent triggering events, it is possible to introduce another triggering function for each vehicle that depends on the information about its state estimate and the state estimates of the neighboring vehicles that communicate with it. With the local information of the states, a new threshold is defined for $\left|e^{[i]}(t)\right|^2$, resulting in the following triggering function:

$$h^{[i]}(t) = \left|e^{[i]}(t)\right|^2 - \left(\theta^{[i]}\frac{\sigma}{\sigma^{[i]}}\sum_{j\in\mathcal{N}^{[i]}} a_{ij}\left(\hat{\gamma}^{[i]}(t) - \hat{\gamma}^{[ij]}(t)\right)^2 + \epsilon_0\right), \tag{15}$$

where a_{ij} represents the adjacency matrix A entries, which take the value of 1 or 0. The other constants: $\sigma, \sigma^{[i]}, \theta^{[i]}$, and ϵ_0 are defined in Hung et al. [2019] and, for the sake of simplicity, were deemed not relevant to show here. Likewise, with the above definition, vehicle i will send its state to its neighbors whenever $h^{[i]}(t) \geq 0$.

4. HYBRID NETWORK – OPTICAL COMMUNICATIONS

Optical communications have narrow directivity patterns, which make the issue challenging when they're added on moving vehicles, whose speeds are consistently being corrected in order to reach consensus. With this in mind, the major goal of this section is to accomplish optical beam alignment between a pair of vehicles. Each vehicle should be able to estimate the position of the neighbors on top of the path they are following, based on the information given by the coordination states. Moreover, it is assumed that the optical modems have an independent rotation axis.

Beam alignment is planned to be accomplished with two phases: rough and refined alignment phases. Rough alignment aims to rotate the beams based on estimates of the positions of each vehicle, which may not lead to proper alignment due to the errors of the estimates. Refined alignment aims to apply small deviations to the rough alignment angle until the beams align, locking that beam orientation.

4.1 Rough Alignment Phase

Let $\boldsymbol{p}_t = [x_t, y_t]^T$ denote the position of the center of mass of the (optical) transmitting vehicle, with a_t denoting the central axis of the transmitting beam and α denoting the angle at which the transmitting beam is oriented. Likewise, let $\boldsymbol{p}_r = [x_r, y_r]^T$ denote the position of the center of mass of the (optical) receiving vehicle, with a_r denoting the central axis of the receiving beam, with orientation given by σ. Fig. 4 represents the geometry of the beam alignment problem.

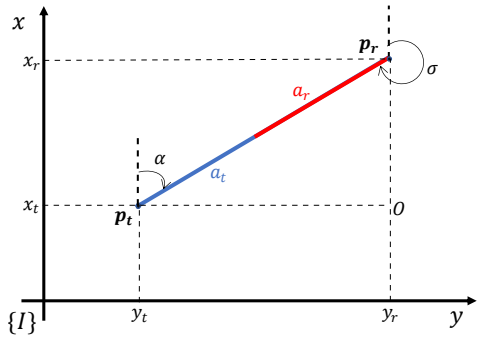

Fig. 4. Geometric representation of the optical beam alignment problem.

For now, it is assumed that each vehicle knows exactly $\boldsymbol{p}_t$ and $\boldsymbol{p}_r$ (and not their estimates). With the goal of overlapping a_t and a_r, a geometric analysis of the situation represented in Fig.4 yields the following equations for α:

$$\alpha(\boldsymbol{p}_t, \boldsymbol{p}_r) = \begin{cases} \frac{\pi}{2} - \arcsin(k), & y_r \geq y_t \\ -\frac{\pi}{2} + \arcsin(k), & y_r < y_t \end{cases}, \tag{16}$$

where k is given by

$$k = \frac{\mathrm{d}(\boldsymbol{O}, \boldsymbol{p}_r)}{\|\boldsymbol{p}_r - \boldsymbol{p}_t\|}. \tag{17}$$

The numerator $\mathrm{d}(\boldsymbol{O}, \boldsymbol{p}_r)$ denotes the signed distance between $\boldsymbol{O}$ and $\boldsymbol{p}_r$. As a result,

$$k = \frac{x_r - x_t}{\sqrt{(y_r - y_t)^2 + (x_r - x_t)^2}}. \tag{18}$$

Similarly, the equations for σ are defined as

$$\sigma(\boldsymbol{p}_r, \boldsymbol{p}_t) = \begin{cases} \frac{3\pi}{2} - \arcsin(k), & y_r \geq y_t \\ \frac{\pi}{2} + \arcsin(k), & y_r < y_t \end{cases}. \tag{19}$$

In order to compute the desired angles for α and σ given in (16) and (19) it requires that the transmitting and receiving vehicles need to exchanges their positions continuously. However, such continuous communication can be avoided by using the estimates of the positions rather than the true ones. This can be done efficiently by making use of the estimate of the coordination states as it is clarified next.

Assume $C^{[t]}$ with a certain j is the path assigned for the transmitting vehicle to follow. The coordinate of the *"reference point"* on the path that the transmitting vehicle must track to achieve path following is denoted by $\boldsymbol{p}_{\mathrm{d}}^{[t]}(s^{[t]}) \in \mathbb{R}^2$, where $s^{[t]}$ is the arc-length of the path. With this notation, the estimate of the transmitting vehicle's position, denoted by $\hat{\boldsymbol{p}}^{[t]}$, can be computed by

$$\hat{\boldsymbol{p}}^{[t]} = \boldsymbol{p}_{\mathrm{d}}^{[t]}(\hat{s}^{[t]}) \in \mathbb{R}^2, \tag{20}$$

where $\hat{s}^{[t]} = L^{[t]}\hat{\gamma}^{[t]}$ with $L^{[t]}$ is the total path length and $\hat{\gamma}^{[t]}$ is the estimate of the coordination state $\gamma^{[t]}$. Note that $\hat{\gamma}^{[t]}$ was computed by the ETC mechanism described in the previous section. This technique is motivated from the fact that if the cooperative path following between the vehicles can be done perfectly then (20) estimates correctly the position of the transmitting vehicle. The estimate of the position of the receiving vehicle can be done analogously.

4.2 Refined Alignment Phase

A refinement is needed because one vehicle may have a wrong idea of the position of its neighbor during a period of time, requiring a small correction to the rough orientations. The correction term applied to desired angle α and σ will work as a sweeping mechanism: sweeping a small neighborhood of each roughly determined angle until the beams align, locking that corrected orientation.

Letting α_c and σ_c denote the corrected angles, defined as

$$\begin{aligned} \alpha_c &= \alpha(\boldsymbol{p}_t, \hat{\boldsymbol{p}}^{[r]}) + A\sin(2\pi f_\alpha t) \\ \sigma_c &= \sigma(\boldsymbol{p}_r, \hat{\boldsymbol{p}}^{[t]}) + A\sin(2\pi f_\sigma t), \end{aligned} \tag{21}$$

where $\hat{\boldsymbol{p}}^{[t]}$ given by (20) ($\hat{\boldsymbol{p}}^{[r]}$ can be computed analogously), f_α and f_σ denote the oscillation frequencies of the correction term in hertz and A denotes the amplitude of the oscillations in degrees, one is capable of sweeping, having used a sine wave with a certain frequency and amplitude as a sweeping term.

One way of determining that refinement has reached its goal and that it was able to correct the orientation is by inspecting the power of the received signal. The power of the signal is largely impacted by how misaligned are the optical beams. The power variation is represented in figure 5.

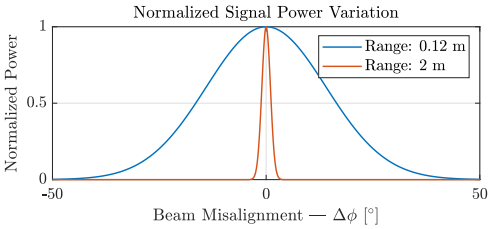

Fig. 5. Variation of the received signal power with the beam misalignment for two different ranges.

In a simulation environment, it is possible to have access to information that in reality each vehicle doesn't have. This is used to compute the ideal orientation for each beam and to evaluate how misaligned the beams are, $\Delta\phi$, during the rough alignment phase. From this, the refinement phase should be activated until the corrected orientation makes the received power be within a user defined threshold.

The following regards should be taken into account:

- The sweeping frequencies should be set according to $f_\alpha = 2f_\sigma$, increasing the chances of beam alignment per period of the sweeping signal with the smallest frequency.
- The amplitude of the sweeping oscillations should start small and then it should increase if, for every two periods of sweeping, beam alignment is not achieved, avoiding situations where small sweepings are not enough.

5. SIMULATION RESULTS

The simulation were set up for three Medusa-class underwater vehicles as in Fig. 6. The simulation parameters can be found in Rego [2021]. Animation of the simulation results can be viewed at `https://youtu.be/wSVyGIrWe5I`.

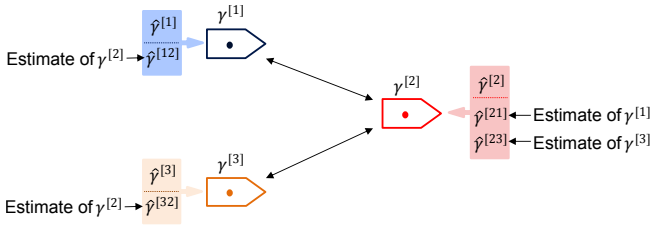

Fig. 6. Adopted communication network between three vehicles. Let $\hat{\gamma}^{[ij]}$ be an estimate of $\gamma^{[j]}$ computed by vehicle i.

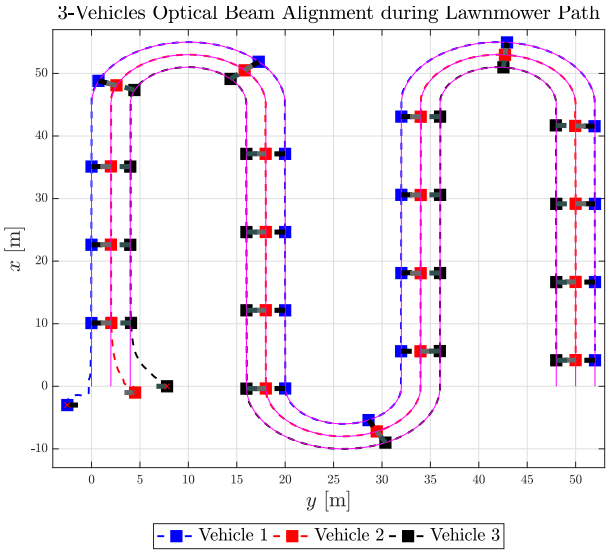

(a) CPF during a lawnmower path.

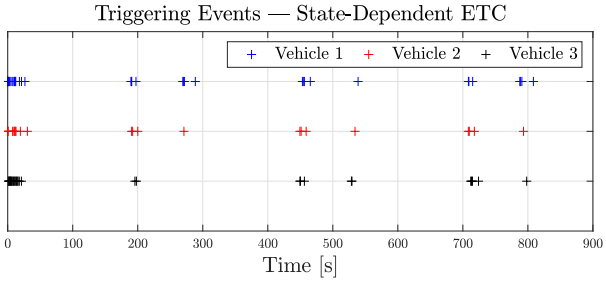

(b) State-dependent triggering events over time.

Fig. 7. Cooperative path following with three vehicles being achieved with acoustic communications.

Fig. 7 shows cooperative path following being achieved with state-dependent ETC. Moreover, it is possible to observe when each vehicle transmits its state, based on the state-dependent triggering function. as it is shown, considering that each vehicle estimates the state of its neighbors, the agents don't need to be communicating continuously to achieve coordination. Additionally, using a triggering function avoids communication congestion when one considers that underwater acoustic communications have slow data transference.

Regarding the proposed mechanism for optical beam alignment between three vehicles, Fig. 8 shows the central axis of each beam reaching alignment during a cooperative mission. With this mechanism, the optical component of the hybrid communication network (acoustic-optical) can

be used to transmit large volumes of data related with the mission among the agents.

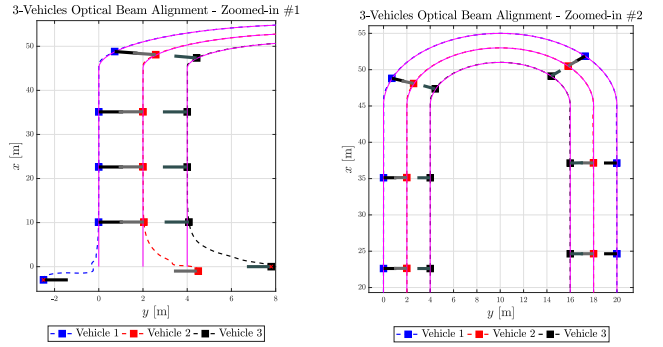

(a) Zoomed-in portion of the path 1.

(b) Zoomed-in portion of the path 2.

Fig. 8. Optical beam alignment for a lawnmower path zoomed-in portions.

Most of the time, the rough alignment phase already produces a good enough orientation of the beams and only a small sweeping is required, as expected by observing Fig. 9. Nevertheless, the refinement phase makes the alignment error be more constrained to a neighborhood of zero, showing that it is an essential phase to make optical communications viable. Ideally, the misalignment represented in Fig. 9 (a) should be kept close to zero for as long as possible, making sure that the beams are aligned for the longest period of time possible. Nevertheless, some oscillations are noticeable due to primarily the refinement mechanism that engages in a sweeping state until the received signal power is adequate for communications.

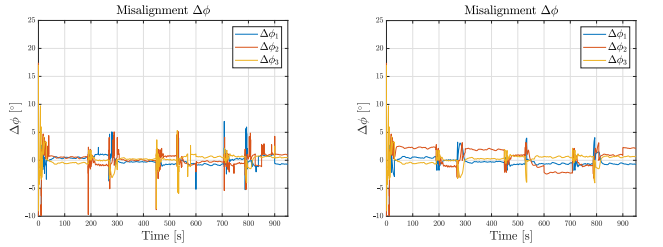

(a) Evolution of the misalignment $\Delta\phi$.

(b) Evolution of the misalignment $\Delta\phi$ without refinement.

Fig. 9. Evolution of the misalignment $\Delta\phi$ with and without refinement.

However, due to the range of communication (2 meters), the power curve is very narrow, as represented before in Fig. 5: even a small deviation can produce a dramatic impact on the value of the received signal power, which is why, the range of communications affects substantially these results (deteriorating as the range increases).

These results show that optical communications can be a viable communication solution for underwater cooperative missions, hence proving that the proposed mechanism works properly. While the refined alignment phase is active, some communication intermittency is to be expected.

6. CONCLUSIONS

The purpose of this work was to ultimately show that using a hybrid communication network, during cooperative missions, is viable. Acoustic communications are commonly used with underwater autonomous vehicles to broadcast the state of the vehicles. However, optical communication modems are just now breaking through in this field and so the problems regarding their narrow directivity patterns boil down to reaching optical beam alignment between a pair of vehicles, which has been shown to be viable.

REFERENCES

Abreu, P.C., Botelho, J., Góis, P., Pascoal, A., Ribeiro, J., Ribeiro, M., Rufino, M., Sebastião, L., and Silva, H. (2016). The medusa class of autonomous marine vehicles and their role in eu projects. In *OCEANS 2016 - Shanghai*, 1–10. doi:10.1109/OCEANSAP.2016.7485620.

Abreu, P.C., Bayat, M., Pascoal, A.M., Botelho, J., Góis, P., Ribeiro, J., Ribeiro, M., Rufino, M., Sebastião, L., and Silva, H. (2015). Formation control in the scope of the morph project. part ii: Implementation and results. *IFAC-PapersOnLine*, 48(2), 250–255. doi:https://doi.org/10.1016/j.ifacol.2015.06.041. 4th IFAC Workshop onNavigation, Guidance and Controlof Underwater VehiclesNGCUV 2015.

Fossen, T.I. (2011). *Handbook of marine craft hydrodynamics and motion control*. John Wiley & Sons.

Ghabcheloo, R., Aguiar, A.P., Pascoal, A., Silvestre, C., Kaminer, I., and Hespanha, J. (2009). Coordinated path-following in the presence of communication losses and time delays. *SIAM journal on control and optimization*, 48(1), 234–265.

Gois, P., Sreekantaswamy, N., Basavaraju, N., Rufino, M., Sebastião, L., Botelho, J., Gomes, J., and Pascoal, A. (2016). Development and validation of blue ray, an optical modem for the MEDUSA class AUVs. In *2016 IEEE Third Underwater Communications and Networking Conference (UComms)*, 1–5. doi:10.1109/UComms.2016.7583455.

Hung, N.T., Rego, F.C., and Pascoal, A.M. (2019). Event-triggered communications for the synchronization of nonlinear multi agent systems on weight-balanced digraphs. In *2019 18th European Control Conference (ECC)*, 2713–2718.

Hung, N.T., Pascoal, A.M., and Johansen, T.A. (2020). Cooperative path following of constrained autonomous vehicles with model predictive control and event-triggered communications. *International Journal of Robust and Nonlinear Control*, 30(7), 2644–2670.

Lapierre, L., Soetanto, D., and Pascoal, A. (2006). Nonsingular path following control of a unicycle in the presence of parametric modelling uncertainties. *International Journal of Robust and Nonlinear Control*, 16(10), 485–503.

Rego, F.C., Hung, N.T., Jones, C.N., Pascoal, A.M., and Aguiar, A.P. (2019). Cooperative path-following control with logic-based communications: Theory and practice. Navigation and Control of Autonomous Marine Vehicles, chapter 8. IET. doi:10.1049/PBTR011E.

Rego, R.T. (2021). *Cooperative Motion Control Using Hybrid Acoustic-Optical Communication Networks*. Master's thesis, Instituto Superior Técnico.

Ribeiro, J. (2011). *Motion control of single and multiple autonomous marine vehicles*. Master's thesis, Instituto Superior Técnico.

Simetti, E., Indiveri, G., and Pascoal, A.M. (2021). Wimust: A cooperative marine robotic system for autonomous geotechnical surveys. *Journal of Field Robotics*, 38(2), 268–288. doi:https://doi.org/10.1002/rob.21986.